International Journal of Earth, Energy and Environmental Sciences
ISSN: 2517-942X
Vol:4, No:6, 2010

Physical-Chemical Surface Characterization of Lake Nasser Sediments

Yousra M. Zakaria Helmy and Edward H. Smith

Abstract**—**Lake Nasser is one of the largest reservoirs in the world. Over 120 million metric tons of sediments are deposited in its dead storage zone every year. The main objective of the present work was to determine the physical and chemical characteristics of Lake Nasser sediments. The sample had a relatively low surface area of 2.9 m^2/g which increased more than 3-fold upon chemical activation. The main chemical elements of the raw sediments were C, O and Si with some traces of Al, Fe and Ca. The organic functional groups for the tested sample included O-H, C=C, C-H and C-O, with indications of Si-O and other metal-C and/or metal-O bonds normally associated with clayey materials. Potentiometric titration of the sample in different ionic strength backgrounds revealed an alkaline material with very strong positive surface charge at pH values just a little less than the pH of zero charge which is ~9. Surface interactions of the sediments with the background electrolyte were significant. An advanced surface complexation model was able to capture these effects, employing a single-site approach to represent protolysis reactions in aqueous solution, and to determine the significant surface species in the pH range of environmental interest.

Keywords**—**Lake Nasser, sediments, surface characterization

I. Introduction

THE Nile River is the longest river in the world. Prior to the construction of the Aswan High Dam, located 15 km south of Aswan city, in 1964, the Nile River flooded annually in August originating from the Ethiopian highlands[1]. This flood was known by its high load of sediments that reached 3700 mg/l [2]. More than 90% of the total average annual suspended load was carried out to the Mediterranean Sea [3]. The construction of the dam resulted in the formation of one of largest man made reservoirs in the world, Lake Nasser.

Lake Nasser (Fig.1) lies between latitude 23°58'N and 20°27'N and longitude 30°07'E and 33°15'E with a total length of the reservoir of about 500 km, 150 km in Sudan (Lake Nubia) and 350 km within the Egyptian boarders[4,5]. The Lake has a total a surface area of 600 km^2 and an average width of 12 km [6]. The total storage capacity of the lake is 160×10^9 m^3, of which nearly 20% is considered to be dead storage (*i.e.* water is not released from this part of the lake regardless of the downstream needs). This zone receives and retains sediments during the flood [6].

Yousra M.Zakaria is with the American University in Cairo, Cairo, AUC Avenue, P.O. Box 74, New Cairo 11835, Egypt (phone: 202-2615-2948; fax: 20.2.2795.7565; e-mail: yousra_m@aucegypt.edu).

Edward H. Smith is with the American University in Cairo, Cairo, AUC Avenue, P.O. Box 74, New Cairo 11835, Egypt (phone: 202-2615-2643; fax: 20.2.2795.7565; e-mail: edsmith@aucegypt.edu).

The amount of sediments deposited in Lake Nasser every year since the full operation of the dam in 1968 is estimated to be over 120 million metric ton [3]. These sediments consist of gravel, sand, silt and clay minerals. The clay minerals in Lake Nasser are montmorillonite, kaolinite and illite [7]. The main objective of the present work is to gain a more quantitative picture of the chemical and physical surface properties of the retained sediments in Nasser Lake. Such information will yield insight into environmentally significant interactions between the sediments and the water column within the lake, and may also indicate potential options for utilizing the sediments once it becomes necessary to remove them from the reservoir.

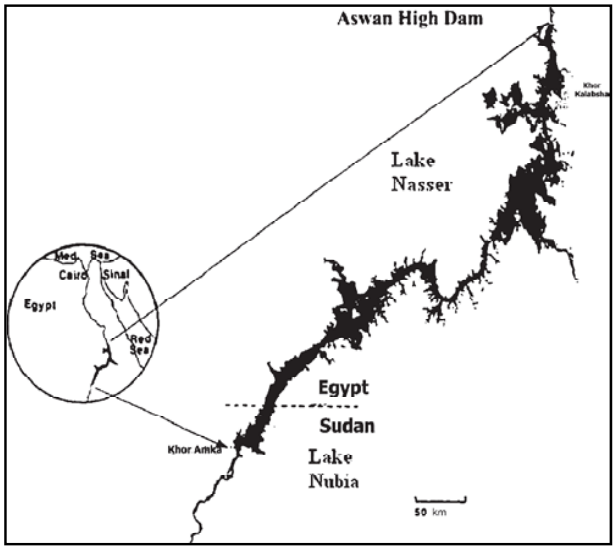

Fig. 1 Lake Nasser Location [used with permission from Springer Science+Business Media: The Nile, Lake Nasser–Nubia, 89, 2009, 126, Gamal M. El-Shabrawy, 1, after Smith, 1990.]

II. Materials and Methods

A. Collection and Processing of Sediments

The sediment sample used in this study was obtained from Nasser Lake in the vicinity of the impoundment at a depth of 18 m. The sample was washed using distilled water several times and left to dry for 48 hours at room temperature. Final drying was at 60 °C in a tray oven.

The dried sample was sieved to different fractions using U.S. standard sieves to determine the grain size distribution. Standard mesh sieve number 200, 100, 80, 50, 40, 30, 20 and 10 were stacked on the top of each other. Mechanical shaking was for 3 minutes followed by collection and measurement of the accumulated weight on each sieve using an analytical

balance. These values were then used in calculating the retained percent weight on each sieve.

A 30/50 fraction sample was chemically activated using 2.0 M H_2SO_4 to evaluate its impact on surface site area. The sample was mixed with the acid at 90°C for three hours and then the mixture was washed with deionized-distilled water three times to assure the removal of any impurities or residuals. After every wash the solution was filtered using a centrifugal separator. Then the sample was left to dry at room temperature.

B. Potentiometric Titration Experiment

Sediment samples from Pass 200 fraction were titrated potentiometrically in ionic background solutions of 0.001 and 0.01 M $NaNO_3$ (in deionized-distilled water) to represent varying solution phase conditions. In the study, 1.0 g of dry sample was suspended in a continuously stirred vessel containing 100 mL of a given electrolyte solution at room temperature. The suspension was purged by nitrogen gas prior to and during the titration. Incremental volumes of standardized 0.1 M NaOH (base) were added precisely using a glass syringe, and the pH recorded using a pre-calibrated pH meter and probe (Schott) every two to ten minutes (so-called, fast titration). Upon achieving pH at least two pH units above the pH of zero salt effect, a freshly-prepared sample at the same electrolyte concentration was titrated with standardized 0.1 M HNO_3 by the same procedure to obtain the acid leg. By this method any hysteresis effects are eliminated. Total volume of acid or base added was less than 2% of the total sample volume.

Supernatant solutions were collected and titrated to observe the influence of substances dissolved from sediments. Sediment was equilibrated overnight in a given electrolyte solution. The solution was then centrifuged followed by filtering through a 0.45 μm membrane to obtain a supernatant free of suspended material. The supernatant and electrolyte only solutions were both titrated using the same procedure described above for the sediment.

C. Chemical Composition Determination

The inorganic composition of the 30/50 fraction of sediments was determined using an energy dispersive X-ray analyzer, EDX, (INCA X-Sight Detector from Oxford Instruments). Furthermore, a number of photographs were taken by a field emission scanning electron microscope, SEM, (Leo Supra 55 from Zeiss with Gemini Column) for the tested samples in order to investigate the surface topography. The sample was tested without pre-treatment.

A Perkin-Elmer 1430 infrared spectrophotometer was used for identification of the characteristic organic functional groups of the 30/50 fraction by Fourier Transform Infrared Spectroscopy (FTIR) using the KBr pellet preparation method. 0.2 g of spectroscopic grade KBr was mixed with 0.002 g of sediment sample, and then a sample pellet was produced by applying pressure using a hydraulic press. The produced pellet was then placed in the microcell adapter for measurement using the infrared spectrometer.

D. Surface Area Measurements

BET surface area of sediment was measured using a Micromeritics (ASAP2020) for a 30/50 fraction sample before and after chemical activation. The measurement had two stages, sample preparation and heating. The sample preparation stage had a temperature rate of 10°C/min and evacuation rate of 20 mm Hg/sec. The heating phase had a hold temperature of 65°C and a hold time of 300 min.

III. Results and Discussion

A. Physical Characteristics

BET surface area of the clayey sediments sample (fraction 30/50) was measured before and after chemical activation and found to be 2.9 m^2/g and 9.16 m^2/g, respectively. The increase in surface area for the post chemical activation sample can be explained by replacing exchangeable cations with H^+ ions leaving SiO_4 groups largely intact and opening up the edges of the platelets [8]. Fig. 2 and Fig 3 show the N_2-isotherm data for the raw and activated sample, respectively, used in BET surface area calculations. As for the shape of particles, the SEM photographs showed high irregularity (Fig. 4).

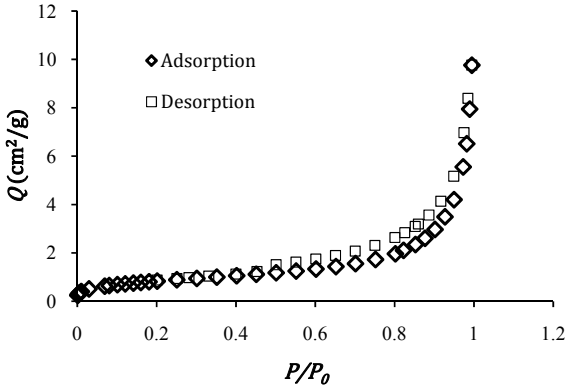

Fig. 2 N_2-isotherm for raw sediment sample (fraction 30/50)

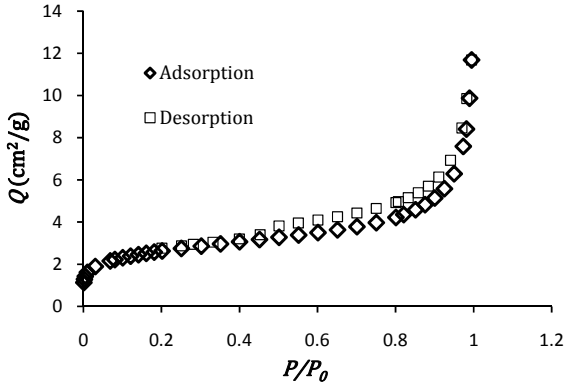

Fig. 3 N_2-isotherm for activated sediment sample (fraction 30/50)

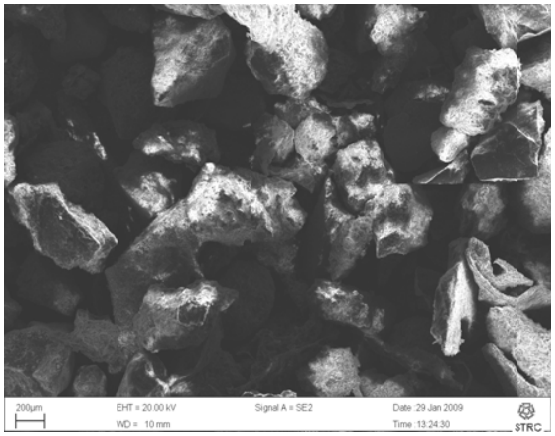

Fig. 4 Raw sediment particles at 223x magnification

B. Grain Size Distribution

Most of the grains had a particle size that ranged between 0.6 and 0.85 mm as most of the sediments sample was retained on sieve 30 as shown in Fig. 5. Also the uniformity coefficient was calculated and it was found to be 4.47.

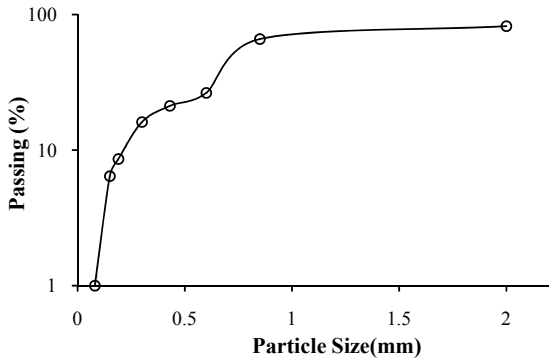

Fig. 5 Particle size distribution for Lake Nasser sediments

C. Chemical Composition

The characteristic organic functional groups and the chemical composition of the sediment sample (30/50 fraction) were determined. The main components of the sample were oxygen, carbon and silicate with a sum weight percent of 85%. There were also some small amounts of calcium, iron and aluminum present as shown in Table 1.

The FTIR analysis, illustrated in the spectrum in Fig. 6, yielded a number of plausible functional groups [9]. The sharp broad band at 3420 cm^{-1} is indicative of O-H in hydroxyl groups. Any remaining water in the sediment could take part in the formation of bonded and non-bonded H-bonds. The small band at 2900 cm^{-1} and its shoulder at 2800 cm^{-1} are normally ascribed to C-H stretching and C-H bending that may indicate the presence of methyl and methylene groups. At 1647 cm^{-1}, the sharp small peak may be C=C vibration in aromatic rings, or C=O stretching in quinines or carboxylic anhydrides. C=O stretching may also be ascribed to the skeletal C=C stretching vibration in the keen peak at 1435 cm^{-1}. This band could also indicate the presence of small concentrations of carbonate. The sharp peak at 1089 cm^{-1} and lesser one at 1036 cm^{-1} likely represent the existence of C-O single bonds associated with carboxylic acids, alcohols, esters, and/or phenols. The peak at 876 cm^{-1} may also be ester-type CH_3-CO- bonds or cyclic C-O-C groups observed in some clays. In general, the keen bands between 876 and 464 cm^{-1} may be attributed to Si-O stretching of O_3SiOH or silicates; or other Metal-C and/or Metal-O bonds that might be expected in clay materials [10].

The chemical composition characterization aided in the functional groups identification by eliminating some options. In the case of wavelength 3420 cm^{-1}, for instance, the options are: O-H, NH_2 and NH. However, the EDX analysis showed that the raw sediments did not contain any nitrogen; hence O-H was the most plausible option.

TABLE I CHEMICAL COMPOSITION FOR RAW SEDIMENT SAMPLE (30/50 FRACTION)

Element	Weight%
C	14.77
O	56.4
Na	0.68
Mg	0.58
Al	2.75
Si	14.19
K	0.9
Ca	6.7
Fe	2.61

D. Potentiometric Titration

Potentiometric titration of the clayey sediment is depicted in Fig. 7 for Pass-200 fraction sediments in 0.01 M $NaNO_3$ background electrolyte solution. Titration curves of reference solutions with the same electrolyte background are included; namely, the electrolyte blank in deionized-distilled water only, and the supernatant containing any dissolved substances from equilibrated sediments. As expected, the titration curve for pure water (with 0.01 M electrolyte) exhibits a rapid pH change at about pH 7. The steep slope was also observed for the supernatant solution in contrast to the relatively shallow slope of the clayey sediment suspension. In fact the supernatant titration curve is almost a perfect trace of the electrolyte blank, suggesting that dissolved species exert a negligible influence on the titration behavior of the clayey sediments. The intersection point of the three curves in Fig. 7 indicates that the pH of zero salt effect (pH_{zse}) is 8.8-9.0. Indeed, the titration experiment revealed that the clayey sediment is an alkaline material as the solution pH increased by as much as 4 pH units when the sample was added to $NaNO_3$ electrolyte solutions in deionized distilled water. The base leg of the titration exhibited a consistent (*i.e.*, monotonic) behavior; however, the acid titration was somewhat irregular owing to the alkaline nature of the material. The apparent high capacity for protons suggests potential applications for the material in adsorbing cations from solution or for cationic exchange reactions with environmentally significant compounds.

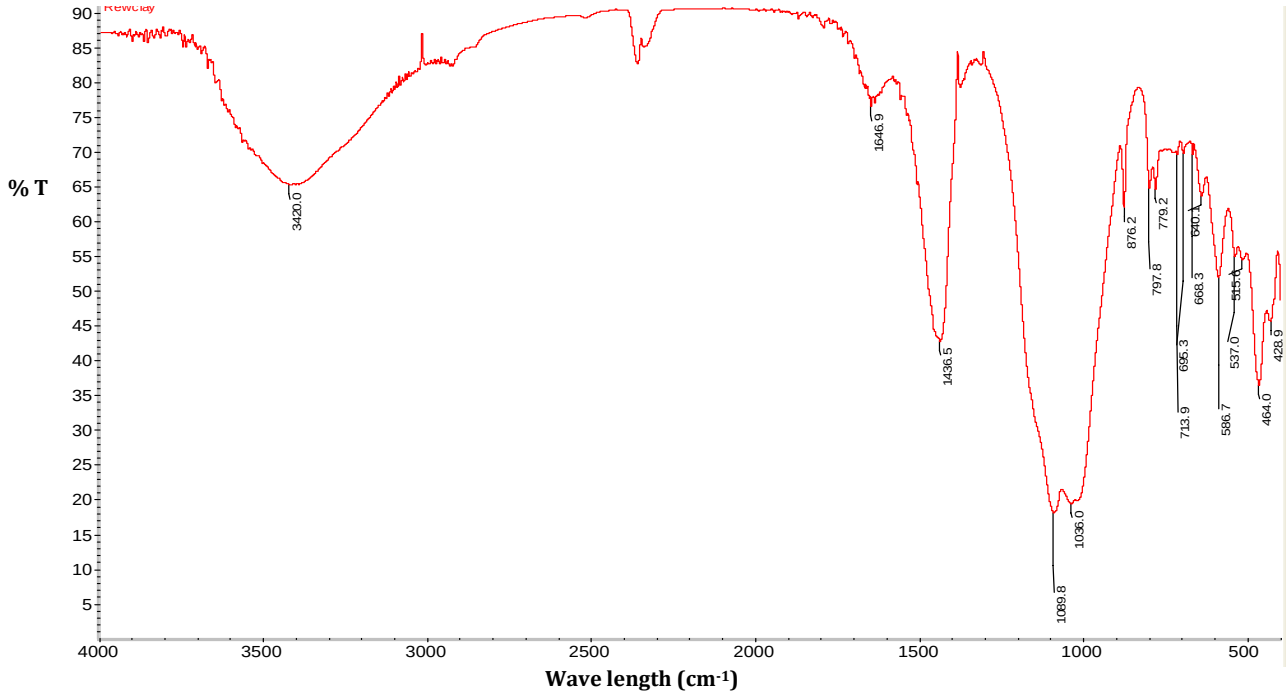

Fig. 6 IR spectrum for clayey sediments (30/50 fraction)

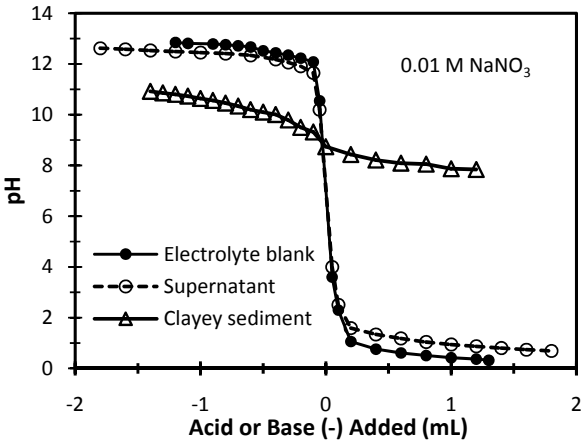

Fig. 7 Potentiometric titration curves of sediment, supernatant, and electrolyte blank solutions in 0.01 M ionic strength at 25 °C

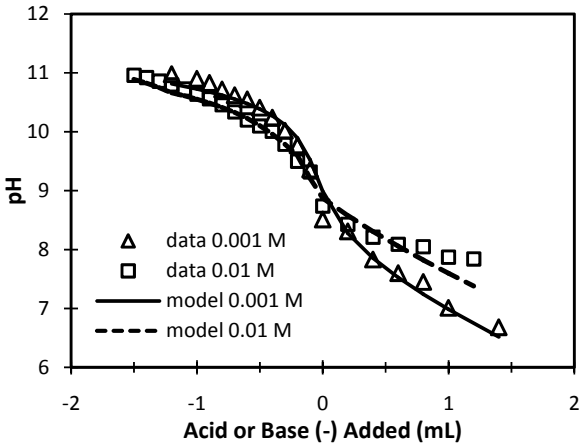

Fig. 8 Potentiometric titration data of clayey sediments at two ionic strengths with TL-SCM simulations

complexation approach that accounts for ionic strength effects on aqueous-surface interactions. The triple layer surface complexation model (TL-SCM) is able to capture these effects in addition to both chemical and electrostatic interactions with ionic aqueous species by providing a more complete depiction of the electrical double layer [11-12]. The following protolysis reactions describe the acid-base chemistry of mineral oxides [13]:

$$> XOH + H^+ \Leftrightarrow > XOH_2^+ \quad (1)$$

$$> XOH \Leftrightarrow > XO^- + H^+ \quad (2)$$

in which the surface species $> XOH_2^+$, $> XOH$, and $> XO^-$ can acquire and/or give up protons in solution.

TL-SCM expressions for the equilibrium constants of reactions (1) and (2), respectively, are:

$$K_1 = \frac{[> XOH_2^+][H^+]}{[> XOH]} \exp\left(\frac{F\psi_o}{RT}\right) \quad (3)$$

$$K_2 = \frac{[> XO^-][H^+]}{[> XOH]} \exp\left(-\frac{F\psi_o}{RT}\right) \quad (4)$$

where K_1 and K_2 are equilibrium constants for the respective surface protolysis reactions, F = Faraday constant (coulombs /mole), R = universal gas constant (cal/°K· mole), T = absolute temperature (°K), and ψ_o = the average potential (volt) of the

inner sphere (or *o*-plane) as given by the Stern-Grahame modification of the Gouy-Chapman description of the electrical double layer [14]. Interactions of electrolyte ions with the postulated surface species are assumed to be weaker-bonded, outer-sphere complexes according to the following reactions with corresponding equilibrium expressions.

$$> XOH + H^+ + NO_3^- \Leftrightarrow (> XOH_2^+ — NO_3^-)$$

$$K_3 = \frac{[> XOH_2^+ — NO_3^-]}{[> XOH][H^+]\,[NO_3^-]} \exp\left(-\frac{F(\psi_\beta - \psi_o)}{RT}\right) \quad (5)$$

$$> XOH + Na^+ \Leftrightarrow (> XO^- — Na^+) + H^+$$

$$K_4 = \frac{[> XO^- — Na^+]\,[H^+]}{[> XOH]\,[Na^+]} \exp\left(-\frac{F(\psi_o - \psi_\beta)}{RT}\right) \quad (6)$$

where ψ_β = the average potential (volt) of the outer, or β, plane. Model calculations also required the measured surface area of the sediments (m^2/g), solid concentration in the titration experiment (g/L), and estimates of the surface site density (sites/nm^2) and linear charge potential (F/m^2). A nonlinear, least squares optimization package, FITEQL [15] was used to estimate the equilibrium constants K_1, K_2, K_3, and K_4 from titration data according to a procedure described previously [11]. Goodness of fit is based on the sum of the squares of the errors between experimental and model values. The plot of titration data at two ionic strengths together with TL-SCM simulations is given in Fig. 8. For this calibration exercise, the log K_i values are:

$\log K_1 = 5.30$ $\log K_2 = -9.20$;
$\log K_3 = 9.90$ $\log K_4 = -10.20$.

Although changing one or more constants may slightly improve the model fit of a given data set, the objective was to obtain a single set of "constants" that capture the effects of variation in background ionic strength.

The pH of zero charge is considered as the intersection pH of successive titration curves and was observed to be 8.8-9 in Fig. 8. This was further confirmed by the surface charge calculation depicted in Fig. 9. The titration data was used to calculate the surface charge variation with solution pH for the pass 200 fraction and ionic background of 0.01 M as $NaNO_3$. As shown in Fig. 9, the sediment surface was positively charged under acidic conditions (approaching a maximum value of 25 C/m^2 at pH 6.8); whereas, it was negatively charged under alkaline conditions (approaching a maximum negative charge of 3.2 C/m^2 at pH 11.5).

Fig. 10 illustrates the speciation of the proposed surface species as a function of pH based upon the equilibria given by equations (3) – (6). Interestingly, >XOH is the only primary surface species that is significant in the pH range of environmental interest. The other prominent surface species is the outer sphere complex (> XOH_2^+ — NO_3^-). The pH-distribution of this species corresponds to the region and magnitude of positive surface charge from Fig. 9, suggesting that electrostatic attraction motivates attachment of NO_3^- to the oxide surface. By contrast, the presence of the other outer sphere complex (> XO^-—Na^+) is not substantial at pH values greater than the pH of zero charge (~9). The magnitude of the negative charge is not sufficient to promote significant electrostatic attraction. Based on much previous research with mineral oxides and even complex clays, it is still possible, even likely, to observe considerable sorption of (especially multivalent) cations as a result of surface complexation with the dominant >XOH surface group according to the following inner-sphere reaction [11,16-17].

$$> XOH + Me^{2+} \Leftrightarrow > XOMe^+ + H^+ \quad (7)$$

where Me^{2+} represents a divalent metal species and >$XOMe^+$ is the corresponding sorbed species. Moreover, the present analysis indicates that surface interactions with background electrolytes are important, necessitating the use of more sophisticated approaches such as the TL-SCM to correctly describe aqueous phase equilibria with environmentally significant substances.

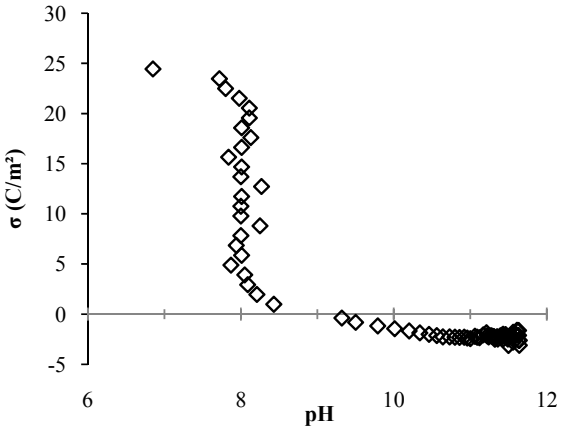

Fig.9 Surface charge distribution for 0.01 M NaNO3 ionic background (pass 200 fraction)

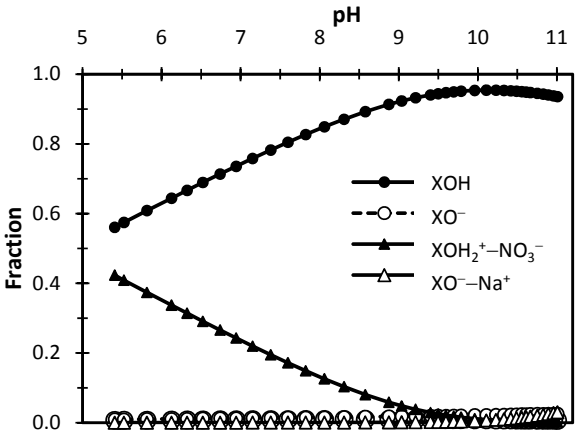

Fig.10 Surface speciation of clayey sediments in 0.01 M $NaNO_3$ from triple layer model calculations using equilibria and constants given in Equations (3)-(6)

IV. Conclusion

Characterization of clayey sediments from Lake Nasser showed that it has a relatively small BET surface area of 2.9 m^2/g which increased to 9.16 m^2/g after chemical activation. Most of the grains had a particle size that ranged between 0.6 and 0.85 mm. The main components of the sample were oxygen, carbon and silicate with some traces of aluminum and iron. The organic functional groups were O-H, C-H, C-O and C=C, with indications of Si-O and other metal-C and/or metal-O bonds normally associated with clayey materials. Potentiometric titration of the sample revealed an alkaline material with very strong positive surface charge at pH values just a little less than the pH of zero charge which is ~9; the magnitude of the negative surface charge at pH > 9 was small by comparison. Surface interactions of the sediments with the background electrolyte were significant. An advanced surface complexation model was able to capture these effects, employing a single-site approach to represent protolysis reactions in aqueous solution. The only primary surface species in the pH range of interest was >XOH; however, this species may undergo relatively strong surface complexation reactions with environmentally significant substances such as multivalent metals. The other prominent surface species is the relatively weaker, outer sphere complex ($> XOH_2^+—NO_3^-$) in which NO_3^- was an anionic electrolyte in solution. The pH-distribution of this species suggests that electrostatic attraction motivates attachment of NO_3^- to the clayey oxide surface.

References

[1] A. A Mageed and M. T Heikal, "Factors affecting seasonal patterns in epilimnion zooplankton community in one of the largest man-made lakes in Africa (Lake Nasser, Egypt)," *Limnologica,* vol. 36, pp.91-97, Nov. 2005.

[2] A. El Gamal, S. Nasr, and A. El-Taher, "Study of the spatial distribution of natural radioactivity in the upper Egypt Nile River sediments," *Radiation measurements,* vol. 42,,pp. 457-465, Feb. 2007.

[3] S. Shalash "Effects of sedimentation on the storage capacity of the High Aswan Dam reservoir," *Hydrobiologia,* vol. 91-92, pp. 623-639. July 1982.

[4] M. M. Ali and M. A. Soltan," Expansion of Myriophyllum spicatum (Eurasian water milfoil) into Lake Nasser, Egypt: Invasive capacity and habitat stability," *Aquatic Botany*, vol. 84, pp. 239-244, Nov. 2005.

[5] M. F. Sadek, M.M. Shahin and C.J. Stigter, "Evaporation from the reservoir of the High Aswan Dam, Egypt: A new comparison of relevant methods with limited data," *Theor. Appl. Climatol.,* vol. 56, pp. 57-66, Mar. 1997.

[6] G. M. El-Shabrawy, "Lake Nasser-Nubia" in *The Nile: Origin, Environments, Limnology and Human Use,* vol.89, H. J. Dumont, Ed. 2009, pp. 125-131.

[7] K. M. Hafiz, "Some quality studies on the sediments of Lake Nasser," M.Sc thesis, Dep. Eng, The American University in Cairo, Cairo, 1977.

[8] K. G. Bhattacharyya and S. S. Gupta, "Adsorption of a few heavy metals on natural and modified kaolinite and montmorillonite: A review," *Advances Coll. Interface Sci.*, vol. 140, pp.114-131, Aug. 2008.

[9] J. Coates, "Interpretation of infrared spectra, a practical approach," in *Encyclopedia of Analytical Chemistry*, R.A. Meyers, Ed. Chichester: John Wiley & Sons, pp. 10815-10837.

[10] A. A. El Hendawy, Personal Communication, March 2010.

[11] E. H. Smith, "Surface complexation modeling of metal removal by recycled iron sorbent," *J. Environ. Engrg. (ASCE)* vol. 124, pp. 913-920, Oct. 1998.

[12] J. A. Davis and D. B. Kent, "Surface complexation modeling in aqueous geochemistry," in *Reviews in Mineralogy – vol. 23: Mineral-water interface chemistry*, M. F. Hochella, Jr. and A. F. White, Eds. Washington D.C.: Mineral. Soc. America, 1990, pp. 177-260.

[13] W. Lu and E. H. Smith, "Modeling potentiometric titration behavior of glauconite," *Geochim.. Cosmochim. Acta*, vol. 60, no. 18, pp. 3363-3373, 1996.

[14] P. W. Schindler and W. Stumm, "The surface chemistry of oxides, hydroxides, and oxide minerals," in *Aquatic Surface Chemistry*, W. Stumm, Ed. New Yorki: John Wiley & Sons, 1987, pp. 83-110.

[15] A. L. Herbelin and J. C. Westall, "FITEQL-version 3.1: A program for the determination of chemical equilibrium constants from experimental data," Oregon State Univ., Corvallis, OR, Report 94-01, Jan. 1994.

[16] D. A. Dzombak and F. M. M. Morel, *Surface Complexation Modeling*, New York: Wiley-Interscience, 1990.

[17] E.H. Smith, W. Lu, T. Vengris, and R. Binkiene, "Sorption of heavy metals on Lithuanian glauconite," *Wat. Res.*, vol. 30, no. 10, 2882-2892, Oct. 1996.